RSC Advances

PAPER

View Article Online
View Journal | View Issue

Cite this: *RSC Adv.*, 2017, **7**, 218

Multistimuli-responsive organogels based on hydrazide and azobenzene derivatives†

Xiaojun Gu,[a] Binglian Bai,*[a] Haitao Wang[b] and Min Li*[b]

The behaviors of organogels of gelators containing hydrazide and azobenzene units connected *via* different flexible central spacers, 1-[4-(4′-methoxylphenylazo)phenoxy]-*n*-[(*N*-(4-nitrobenzoyl)-*N*′-(benzoyl-4′-oxy)hydrazine)]alkane (**E*n***, n = 5, 6, 10) have been studied. The length and parity of the central flexible spacer play crucial roles in the gelation. **E6** and **E10** could form a stable organogel in DMF, and the critical gelation concentration of **E10** is higher than that of **E6**, but no gelation is observed for compound **E5**. Xerogels of **E6** and **E10** from DMF exhibited fibrous aggregates. The organogels showed a photoinduced gel-to-precipitate transition under the irradiation by UV light irradiation, which was attributed to the photoisomerization of azobenzene. The *trans–cis* isomerization in gels further caused the morphological change from fibrous to globular aggregates. In addition, the organogel exhibited multiple stimuli-responsive behaviors upon exposure to stimuli such as temperature, anions and pH.

Received 8th October 2016
Accepted 2nd November 2016

DOI: 10.1039/c6ra24886a

www.rsc.org/advances

1. Introduction

Low molecular weight organogels (LMWGs) which were driven by non-covalent interactions including hydrogen bonds, hydrophobic interactions, π–π interactions and van der Waals forces have attracted considerable attention as a key class of soft nanostructured material.[1–4] Recently, numerous efforts have been devoted to the development of stimuli-responsive gels, whose properties can be either switched on–off or tuned in the presence of an external or internal chemical or physical stimulus such as light,[5,6] pH,[7–9] ultrasound,[10,11] or ionic stimuli.[12,13]

Supramolecular organogels and liquid crystals are fascinating organized self-assembled soft materials.[14] Liquid crystal dimers are composed of molecules containing two conventional mesogenic groups linked *via* a flexible spacer. These materials show quite different behavior to conventional low molar mass liquid crystals and in particular their transitional behavior exhibits a dramatic dependence on the length and parity of the flexible spacer.[15] We have reported that the unusual mesophase of liquid crystal dimer **E*n*** (Scheme 1),[16] **E6** and **E10** exhibit enantiotropic SmA phase, while **E5** is non-mesomorphic. In addition, the melting point of **E5** is much lower than that of **E6**, which indicated the characteristic odd–even effect in **E*n***. Recently, we reported that the effect of flexible central spacer on the *trans–cis* photoisomerization of azobenzene organogels.[17] However, to date, there is no report of the length and parity of the central flexible spacer effect on the properties of organogels.

Our present paper focused on the gelation behavior, photo-responsive, anion-responsive and pH-responsive behavior of **E*n*** (Scheme 1). The results of these studies contribute to further understanding the structure–property relationships of LMOGs.

2. Experimental

2.1 Characterization

Xerogels were prepared by freezing and pumping the organogel of **E6/E10** for 3 days. Field emission scanning electronicmicroscopy (FE-SEM) observations were recorded with a SSX-550 apparatus. X-Ray diffraction (XRD) was carried out on a Bruker Avance **E6/E10** X-ray diffractometer. The xerogels were pressed into a tablet with KBr for the Fourier transform IR spectrum (FTIR) measurements. Differential scanning calorimetry (DSC) curves were obtained on a Netzsch DSC 204 instrument. The UV irradiation was carried out with a 500 W Xe lamp with bandpass filter (280–375 nm).

^{1}H-NMR spectra were recorded with a Bruker Avance 500 MHz spectrometer and Mercury-300BB 300 MHz spectrometer using dimethyl sulfoxide-d as a solvent and tetramethylsilane (TMS) as an internal standard (δ = 0.00). UV-vis absorption spectra were recorded on a Shimadzu UV-2550 spectrometer.

Spectrophotometric titrations were performed on solutions of receptors in DMF at room temperature. Anions (F^-, Cl^-, Br^-, I^- and AcO^-) and NaOH were used in solution by adding the relative alkylammonium salts.

[a]*Key Laboratory of Coherent Light and Atomic and Molecular Spectroscopy of Ministry of Education, College of Physics, Jilin University, Changchun 130012, PR China*
[b]*Key Laboratory for Automobile Materials (JLU), Ministry of Education, College of Materials Science and Engineering, Jilin University, Changchun 130012, PR China. E-mail: weijue@jlu.edu.cn; minli@mail.jlu.edu.cn; Tel: +86-431-85168254*

† Electronic supplementary information (ESI) available. See DOI: 10.1039/c6ra24886a

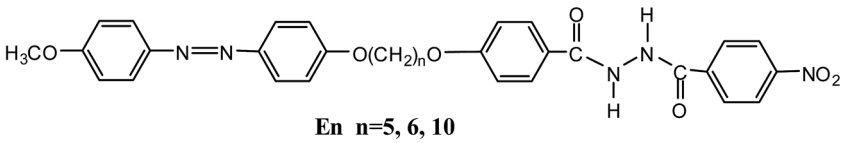

Scheme 1 Molecular structure of compounds E*n*.

3. Results and discussion

The compounds **E*n*** were synthesized in our laboratory, and their structures were confirmed by FTIR, ^{1}H-NMR spectroscopy and elemental analysis. The synthetic details were reported elsewhere.[16]

3.1 Gelation behaviors

The gelation abilities of **E*n*** were evaluated in various organic solvents by the standard heating and cooling method. The compounds **E*n*** were insoluble in aliphatic hydrocarbon solvents, lower alcohols and aromatic solvents, such as *n*-hexane, cyclohexane, chloroform, methanol and toluene by heating, but were easily dissolved in *N*, *N*-dimethylformamide (DMF), dimethyl sulfoxide (DMSO) and tetrahydrofuran (THF). **E6** and **E10** could form stable organogel in DMF, and the critical gelation concentrations (CGC) of **E10** (11.5 mg mL^{-1}) is higher than that of **E6** (8 mg mL^{-1}), it indicates that **E6** gelation is more efficient than **E10**, but no gelation is observed for compound **E5** (Table S1†). This behavior may be most attributed to the dependence of the molecular shape on the parity of the spacer considered in the all-*trans* conformation. In **E6**, with an even numbered spacer (Fig. S1a†), the molecules are disposed to give an overall rodlike shape, whereas in **E5**, with an odd-numbered spacer (Fig. S1b†), the molecules are inclined with respect to each other giving a bent-shaped motif. The structure of **E6** with even-numbered spacer is considered to be more compatible with the molecular organization.[15] Meanwhile, the dipole moment value of **E5** with bent-shaped motif increases, which improves the solubility of the **E5** in DMF (polar solvent) and thus disturbs the aggregation of the **E5** molecules, so the increase of the dipole moment value may be another reason for the gelation behavior. Fig. S2† shows the gel–sol transition temperature (T_{gel}) of the **E6** and **E10** gels in DMF as a function of concentration.

The aggregation morphologies of **E*n*** were investigated by scanning electron microscopy (SEM). As shown in Fig. 1, the **E6** and **E10** xerogel showed 3D network, in which rigid (**E6**) and flexible (**E10**) fibers with the width of 0.5–2 μm were observed, while the concentrated solution of **E5** consists of flat ribbons 2.7–3.0 μm wide (Fig. S3†). The formation of fibers or ribbons indicates that the self-assembly is driven by strong directional intermolecular interactions.

The rheological properties of the **E6** and **E10** gel were shown in Fig. S4.† The frequency sweep experiment (Fig. S4b and d†) of the gel reveals that $G' > G''$ and is independent of the frequency in a wide frequency region, indicating the gel nature of the sample. Stress sweep experiments (Fig. S4a and c†) of the gel indicate that the G' and G'' cross each other at an oscillator stress of 10 Pa, indicating the breaking of the gel to a sol state.

As shown in Fig. 2, FTIR spectroscopy of the **E6** xerogel from DMF showed hydrogen-bonded N–H stretching vibrations at around 3280 cm^{-1}, free C=O at around 1701 and hydrogen-

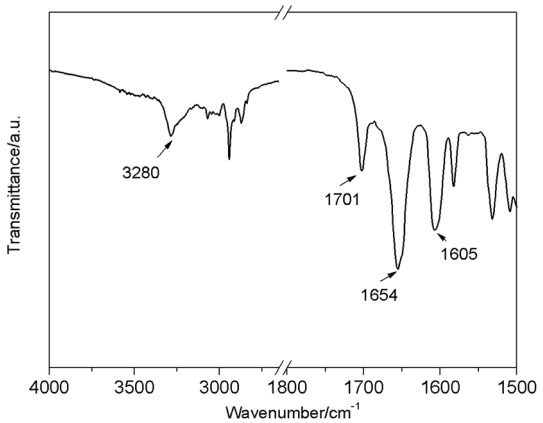

Fig. 2 FTIR spectrum of **E6** xerogel (8 mg mL^{-1}) in DMF.

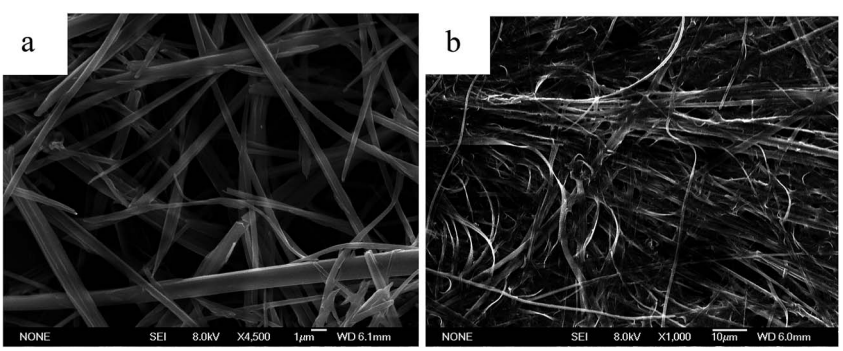

Fig. 1 SEM images of (a) **E6** xerogels (8 mg mL^{-1}); (b) **E10** xerogels (11.5 mg mL^{-1}) in DMF.

bonded C=O at around 1654 cm^{-1}, indicating that the N–H groups were mostly associated with C=O groups *via* N–H···O=C hydrogen bonding in the xerogel.[18]

In order to get more structural information, the xerogels were subjected to powder X-ray diffraction. As shown in Fig. 3, the XRD pattern of the **E6** DMF xerogel exhibited sharp peaks in the lower-angle region with the *d*-spacings of 35.3 nm, 17.9 nm and 11.6 nm, respectively, illustrating that a lamellar organization with the interlayer distance of 3.53 nm in the gel phase, which is slightly shorter than the calculated molecular length (l = 3.68 nm) of the most extended conformation, while it is same as that of SmA_1 mesophase of **E6**.[16] In the large angle range, a peak around $2\theta = 25.1°$ (0.35 nm) is characteristic of a typical π–π stacking distance.[17,19]

3.2 Photo-responsive properties

As shown in Fig. 4, when the gel of **E6** was exposed to UV light irradiation, the gel collapsed gradually and finally precipitates were observed. But this state did not change upon photo-irradiation by visible light irradiation, and the gel phase could not be restored by heating.

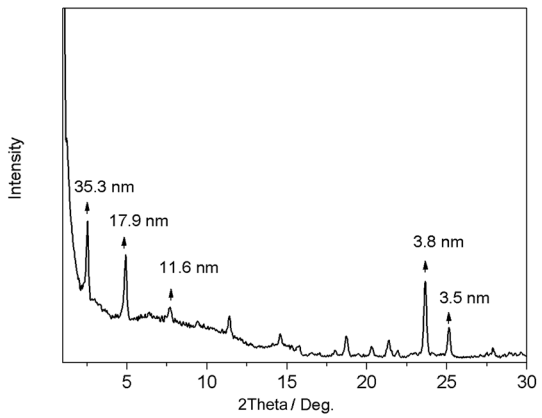

Fig. 3 X-Ray diffraction pattern of xerogel from **E6** (8 mg mL^{-1}) in DMF.

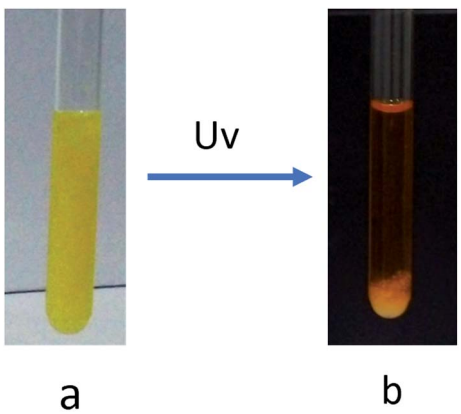

Fig. 4 Photographs of the DMF gel of **E6** (8.0 mg mL^{-1}) before (a) and after (b) UV light irradiation for 9 h.

The UV light irradiation also caused the morphology change of the **E6** gel. Compared to the fibrous aggregates of the xerogel in DMF (Fig. 1a), SEM image of the precipitates after UV light irradiation showed some fibers adhered some globular aggregates with diameters of 1–2 μm (Fig. 5a), whereas the cast film of the solution (developed from the gel in DMF under the UV light irradiation) showed globular aggregates, no fibers (Fig. 5b). The SEM image of the cast film of the solution after visible light irradiation on the basis of UV irradiation exhibited some globular aggregates adhered with each other (Fig. 5c).

This phase transition can be further confirmed by monitoring the UV-vis spectroscopy evolution of **E6** solution in DMF (1×10^{-3} mol L^{-1}). The UV-vis spectroscopy (Fig. 6a) showed the typical change, the intensity of the π–π* absorption peak of the *trans*-azobenzene moieties at 358 nm decreased with the UV light irradiation time, while that of the n–π* absorption peak of the *cis*-azobenzene at 448.5 nm increased concomitantly, indicating that photoinduced *trans–cis* isomerization took place and eventually brought about the gel–precipitate transition. Fig. S9† showed the reversibility in the photoisomerization by alternate irradiation of UV and visible light. The conversion efficiency of *cis*-azobenzene reached *ca.* 87% at the photo-stationary state within 18 s, estimated from the UV-vis absorption spectra (Fig. 6a), whereas the *trans*-azobenzene only can be recovered *ca.* 51% at the photo-stationary state within 9 s (Fig. 6b). The *trans*-azobenzene cannot be all recovered was also confirmed by the ^{1}H-NMR under irradiation by 450 nm visible light (Fig. S10c†), but the *trans*-azobenzene can be recovered by heating (Fig. S10d†) or place in darkness enough time after UV or visible light irradiation (Fig. S11†).

The FTIR spectrum of **E6** in the precipitate (developed from the DMF gel under the UV irradiation) (Fig. 7a) showed characteristic bands of N–H stretching modes of amide groups at 3240 cm^{-1}, which is 40 cm^{-1} shorter than that in the gel state. In addition, the C=O stretching vibration shifted from 1701 cm^{-1} and 1654 cm^{-1} (gel state) to 1654 cm^{-1} (precipitate). It is obviously that the intermolecular hydrogen bonding between N–H and C=O in the precipitate was stronger than that in gel state (Fig. 7b).

Combining the above results, we proposed a possible mechanism of photoinduced gel–precipitation change. **E6** molecules in the gel state are dominantly in the *trans*-conformation, which self-assembled to layered aggregation to form the stable gel, and the main driving forces for gelation were intermolecular hydrogen bonding between the hydrazide groups and π–π interactions between the azobenzene groups. Meanwhile there exists the equilibrium among the assembled fibrous network and the dissolved small assemblies and the molecularly dispersed *trans*-**E*n***. Irradiation of the gel by UV light firstly leads to *trans–cis* isomerization of the azobenzene units in the dissolved assemblies and the molecularly dispersed *trans*-**E*n***. In the *cis*-isomers the dipole moment value increases, which improves the solubility of the **E6** in DMF (polar solvent). With the increase of irradiation time, a certain amount of *trans*-isomers in fiber of organogel also turns into *cis*-isomers and then dissolves, thus the concentration of *cis*-isomers increases and further globular aggregates form. Meanwhile, the rest of

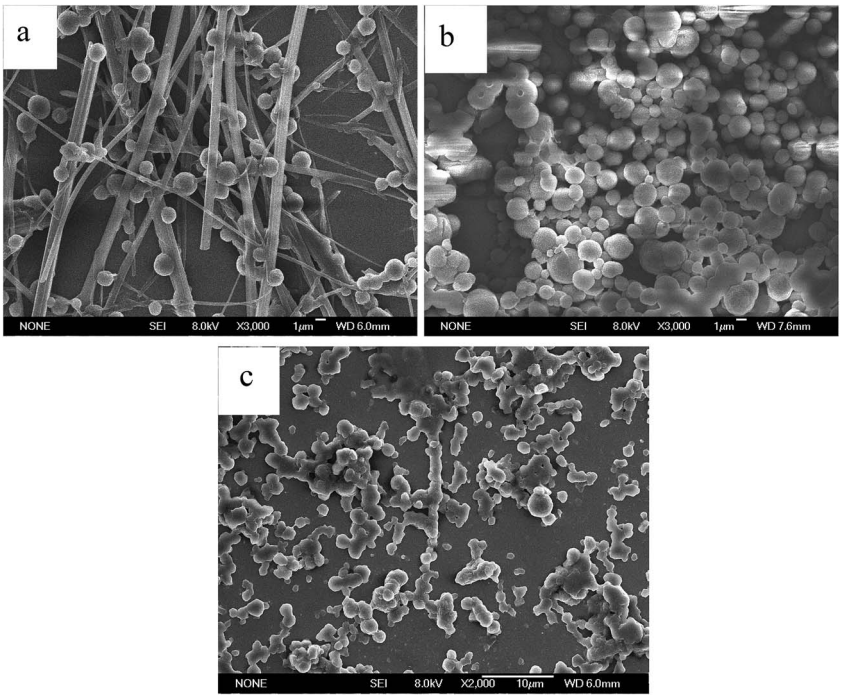

Fig. 5 SEM images of **E6** (8 mg mL^{-1}): (a) the precipitate and (b) the cast film of the solution (developed from the gel in DMF under the UV light irradiation); (c) the cast film of the solution after visible light irradiation on the basis of UV light irradiation.

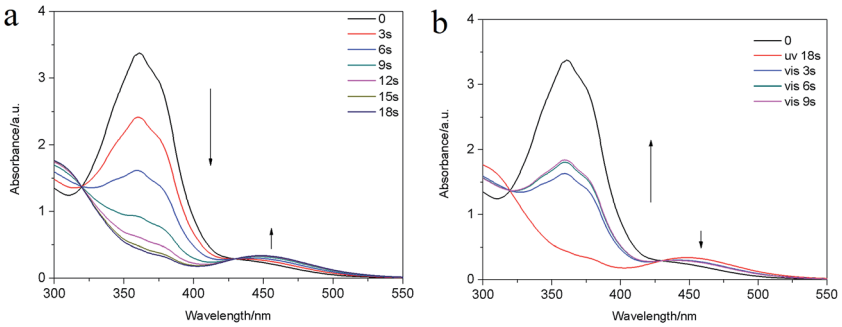

Fig. 6 UV-vis spectra of **E6** solution in DMF (1×10^{-3} mol L^{-1}) (a) under UV light irradiation for 0–18 s; (b) under visible light irradiation for 0–9 s.

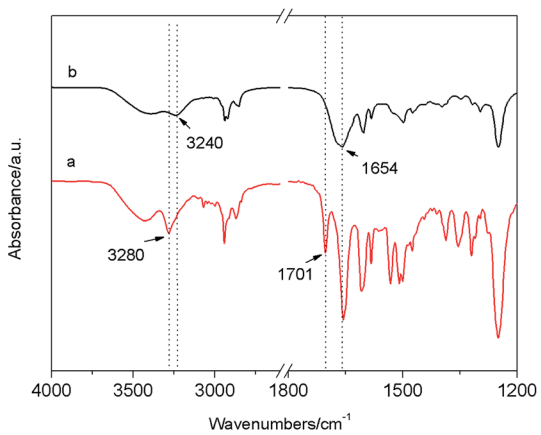

Fig. 7 FTIR spectra of (a) xerogel of **E6** in DMF; (b) the precipitate developed from the gel in DMF under the irradiation of 365 nm UV light for 9 h.

fiber of *trans*-isomers in original organogel cannot support the large volume of organic liquid, so results in the organogel disintegrating and some fiber of *trans*-isomers precipitated out simultaneously.

3.3 Anion responsive properties

The use of these low molecular weight organogels as sensors for various anions (F^-, Cl^-, Br^-, I^-, AcO^-, as $[Bu_4N]^+$ salt) was examined in DMF. The presence of F^- and AcO^- not only changes the color of the systems, but also disrupts the preformed gel into a solution through slow diffusion of the anion, while gel remained upon addition of the other halide anions (Fig. 8). The absorption spectra of **E6** in DMF (Fig. 9) in the presence of various anions showed intense variation upon the addition of F^- and AcO^- at room temperature. The new absorption bands at 451 nm are responsible for vivid color changes.

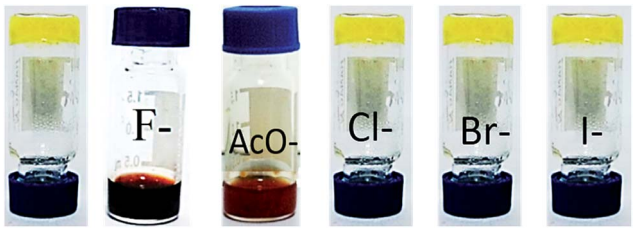

Fig. 8 Photograph of **E6** organogels (8 mg mL^{-1}) upon adding of 10 equiv. of various anions in DMF, from left to right: none, F^-, AcO^-, Cl^-, Br^-, I^-.

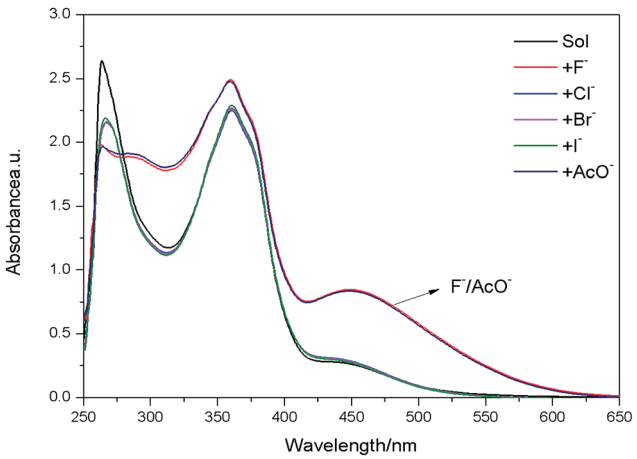

Fig. 9 UV-vis spectra of **E6** (1×10^{-4} mol L^{-1}) in DMF upon addition of 10 equiv. of various anions (F^-, Cl^-, Br^-, I^-, AcO^-).

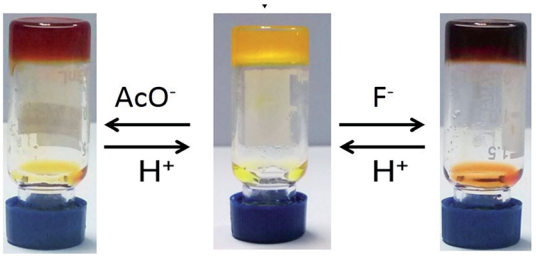

Fig. 10 Reversible gel–gel color transition of the two-components gel of **4-poxd-B8** and **E5** (the molar ratio 1 : 1) in DMSO triggered by F^- and AcO^-.

The evidence for the anion-responsive mechanism was obtained from ^{1}H NMR experiments in DMSO-d_6 in Fig. S17,† the addition of 5 equiv. F^- resulted in the disappearance of the signals at 10.46 ppm and 10.64 ppm of the NH protons, and the appearance of a weak signal at δ = 10.44 ppm, indicating the formation of N–H···F^- hydrogen bond, simultaneously, a new weak signal appeared at δ = 15.71 ppm, which implied the formation of a stable bifluoride hydrogen-bonding self complex (HF_2^-)[20–22] and the occurrence of bifluoride points to the deprotonation of either the N–H group. After addition of 3 equiv. of AcO^- ions, the NH signal disappeared, suggesting that only a hydrogen-bond complex [**E*n***·AcO]$^-$ is observed in Fig. S18.†

In addition, the gel–gel colorimetrical sensor can be obtained through two-component organogel based on **E5** and **4-poxd-B8** gelator in the Fig. 10 (the molar ratio 1 : 1, the molecular structure of **4-poxd-B8** was shown in Fig. S19†[23,24]). As shown in Fig. S20, S21, S23 and S24,† the UV-vis and ^{1}H NMR spectra indicate that there is no interaction between the **4-poxd-B8** and **E5**, as well as the **4-poxd-B8** and F^-. The presence of F^- can not disrupt the preformed gel into a solution through slow diffusion of the F^-, only can change the color of the two-component organogel (Fig. 10). The F^- only can interact with **E5**, the role of the **4-poxd-B8** is to form 3D cross-linking network by self-assembling to support the solvent to form organogel and keep the organogel without disassembly in the presence of F^-, which is in agreement with the morphology as shown in Fig. S22.†

3.4 pH responsive properties

Similar to the F^- response, reversible gel–sol transition induced by deprotonation and protonation steps by the addition of a base and an acid, respectively. Upon addition of 10 equiv. solid NaOH onto the top of the **E*n*** DMF gel at room temperature, a thin layer of black solution immediately appeared at the upper part. As time passed, all the yellow gel transferred into black solution through slow diffusion of the NaOH (Fig. S25b†). When the HCl was added into the black solution formed by the NaOH disintegrated gel, a new organogel formed again (Fig. S25c†). The UV-vis spectroscopic (Fig. 11) and ^{1}H NMR titration

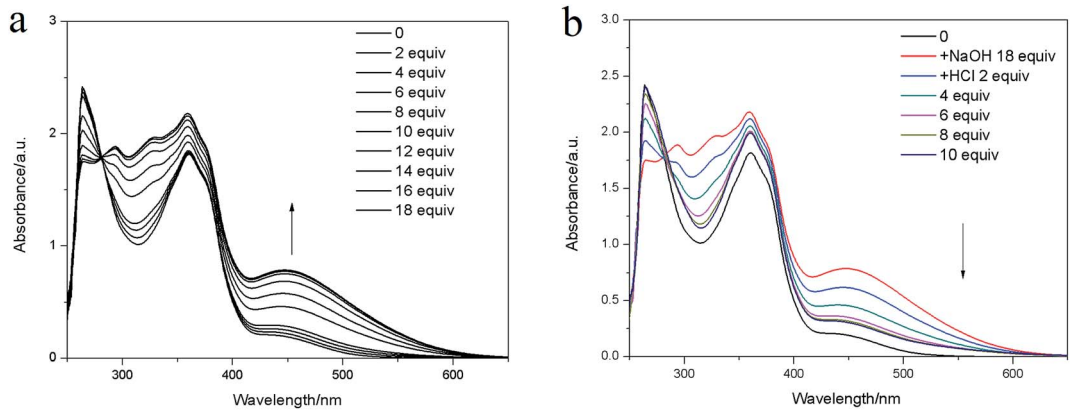

Fig. 11 UV-vis absorption spectra of **E6** in the presence of (a) NaOH (0–18 equiv.); (b) HCl in DMF (1×10^{-4} mol L^{-1}).

experiments (Fig. S26†) also confirmed the pH-responsive phenomenon.[7–9,25]

4. Conclusion

In conclusion, the gelation behaviors of **E*n*** were studied. It was maybe due to the effect of the different molecular shape of **E*n*** with the odd or even numbered central spacer, **E6** and **E10** could form stable organogel in DMF, but no gelation is observed for compound **E5**. The organogels exhibited multiple stimuli-responsive behaviors upon exposure to a number of environmental stimuli including temperature, light, anion and pH. Upon irradiation with UV light, the organogels showed photo-induced gel-to-precipitate transition and morphological changed from fibrous to globular aggregates. Upon addition of anion (F^- and AcO^-) or base (NaOH), the gel can show both color change and gel–sol transition. The results of these studies can further understand the structure–property relationships of LMOGs.

Acknowledgements

This work was supported by the National Natural Science Foundation of China (21072076), the Project of Science and Technology Development Plan of Jilin Province (20140414020GH) and Project 985-Automotive Engineering of Jilin University.

References

1 J. M. Lehn, *Science*, 1993, **260**, 1762–1763.
2 J. M. Lehn, *Supramolecular chemistry: concepts and perspectives*, Wiley-VCH, Weinheim, 1995.
3 M. George and R. G. Weiss, *Acc. Chem. Res.*, 2006, **39**, 489–497.
4 P. Terech and R. G. Weiss, *Chem. Rev.*, 1997, **97**, 3133–3160.
5 C. T. Chen, C. H. Chen and T. G. Ong, *J. Am. Chem. Soc.*, 2013, **135**, 5294.
6 M. Moriyama, N. Mizoshita, T. Yokota, K. Kishimoto and T. Kato, *Adv. Mater.*, 2003, **15**, 1335.
7 D. Y. Jeon, W. J. Yoo, S. H. Shin, *et al.*, *Journal of Sensor Science and Technology*, 2012, **21**(3), 223–228.
8 S. Islam, N. Bidin, S. Riaz, *et al.*, *Sens. Actuators, A*, 2016, **238**, 8–18.
9 K. Kimura, S. Yajima, H. Takase, *et al.*, *Anal. Chem.*, 2001, **73**(7), 1605–1609.
10 T. Naota and H. Koori, *J. Am. Chem. Soc.*, 2005, **127**, 9324–9325.
11 G. Cravotto and P. Cintas, *Chem. Soc. Rev.*, 2009, **38**, 2684–2697.
12 K. Kimura, S. Yajima, H. Takase, *et al.*, *Anal. Chem.*, 2001, **73**(7), 1605–1609.
13 S. H. Lee, J. Sumranjit, P. Tongkate, *et al.*, *Electrochim. Acta*, 2014, **123**, 198–204.
14 N. M. Sangeetha and U. Maitra, *Chem. Soc. Rev.*, 2005, **34**, 821–836.
15 C. T. Imrie, *Struct. Bonding*, 1999, **95**, 149–192.
16 B. L. Bai, H. T. Wang, P. Zhang, S. N. Qu, F. Li, Z. X. Yu, B. Long and M. Li, *Liq. Cryst.*, 2008, **35**, 793–798.
17 B. L. Bai, M. G. Zhang, J. Wei, H. Y. Yan, H. T. Wang, Y. Q. Wu and M. Li, *Tetrahedron*, 2016, **72**, 5363–5368.
18 P. I. Harris and D. Chapman, *Biopolymers*, 1995, **37**, 251–263.
19 B. L. Bai, X. Y. Mao, J. Wei, Z. H. Wei, H. T. Wang and M. Li, *Sens. Actuators, B*, 2015, **211**, 268–274.
20 Y. Zhang and S. Jiang, *Org. Biomol. Chem.*, 2012, **10**(34), 6973–6979.
21 L. Wang, W. Wei, Y. Guo, *et al.*, *Spectrochim. Acta, Part A*, 2011, **78**(2), 726–731.
22 J. W. Liu, Y. Yang, C. F. Chen, *et al.*, *Langmuir*, 2010, **26**(11), 9040–9044.
23 C. X. Zhao, H. T. Wang, X. Ran, B. L. Bai, Y. Zhang and M. Li, *Chin. J. Chem.*, 2012, **30**, 785–790.
24 C. X. Zhao, H. T. Wang, B. L. Bai, S. N. Qu, J. X. Song, X. Ran, Y. Zhang and M. Li, *New J. Chem.*, 2013, **37**, 1454–1460.
25 T. A. Khattab, B. D. B. Tiu, S. Adas, S. D. Bunge and R. C. Advincula, *Dyes Pigm.*, 2016, **130**, 327–336.